IEEE Access
Multidisciplinary | Rapid Review | Open Access Journal

Received November 27, 2018, accepted February 15, 2019, date of publication February 28, 2019, date of current version March 18, 2019.

*Digital Object Identifier 10.1109/ACCESS.2019.2902316*

# Effective Geometry Monte Carlo: A Fast and Reliable Simulation Framework for Molecular Communication

**FATIH DINÇ, MATIJA MEDVIDOVIĆ, AND LEANDER THIELE**
Perimeter Institute for Theoretical Physics, Waterloo, ON N2L 2Y5, Canada

Corresponding author: Fatih Dinç (fdinc@perimeterinstitute.ca)

Research at the Perimeter Institute is supported by the Government of Canada through the Department of Innovation, Science and Economic Development Canada, and by the Province of Ontario through the Ministry of Research and Innovation.

**ABSTRACT** Angular information of messenger molecules absorbed by a receiver plays a significant role in the molecular communication literature. In this paper, we address systematic biases and random errors in the angular information stemming from finite step sizes encountered in traditional simulation frameworks. We show that the effective geometry Monte Carlo (EG-MC) simulation algorithm, which modifies the geometry of the receiver, is a fast and reliable simulation method to overcome these systematic biases. We motivate our approach for a 3-D unbounded diffusion channel consisting of an absorbing receiver and a point transmitter. We show that, with minimal computational cost, the angular distribution of the absorbed particles by the receiver can be precisely obtained using EG-MC algorithm. Afterwards, we demonstrate the accuracy of our simulations and compare them to traditional methods. Then, we comment on the range of applicability of our results. Finally, we consider two simple cases with constant flow and show that the EG-MC algorithm gives consistent results even when the drift is dominant over diffusion. We conclude with further remarks on the computational efficiency and reliability of the EG-MC method.

**INDEX TERMS** Effective geometry Monte Carlo simulations, molecular communication, diffusion channels, spherical absorbing receivers.

## I. INTRODUCTION

Molecular communication via diffusion is growing in interest due to its applications in nano-science and health-related fields [1]–[5], especially for describing communication between nano-machines. This communication is performed by messenger molecules that are used to mediate the signal between receivers and transmitters in a diffusion channel. As many proposed nano-machines are biocompatible, there have been many biology-related applications of molecular communication [6]–[9]. Therefore, examining communication characteristics and communication scenarios is of substantial importance for further developments in this area. Two types of receivers are commonly considered in molecular communication literature: absorbing receivers that consume incoming molecules, or observing receivers that track the number of molecules inside a volume without absorbing them. Analytical results for simple cases, such as a spherical absorbing receiver inside a 3-D diffusion channel [10], [11] have been obtained. For more complicated systems, simulations and semi-analytic approaches have been utilized [12]–[17].

Many different simulation frameworks for molecular communication have been proposed in the literature, such as N3Sim [18], NanoNS [19], BiNS2 [20], AcCoRD [21] and nanoNS3 [22]. The most commonly used simulation algorithm is the so called Monte Carlo (MC) Algorithm. In this algorithm, each step consists of two main events. First, the molecules freely diffuse inside the channel in-between time steps. Then, a receiver absorbs the molecules in the vicinity of its boundary [23]. This algorithm has been proven to perform quite accurately for small step sizes and is used extensively in the literature. Nonetheless, the price for high accuracy is high computation power, i.e. iteration number, that is required to simulate complex systems. Increasing the step size can cause significant problems in the simulation, one of which is called the intra-step

The associate editor coordinating the review of this manuscript and approving it for publication was Daniel Benevides da Costa.

absorption problem. This effect is well-understood in the molecular communication literature and various solutions were proposed [21], [24], [25]. The main focus of the literature has been to solve this problem using different absorption models approximating the molecule behavior near the receiver boundary (refined Monte Carlo Simulations (RMC) in [24] and a priori Monte Carlo simulations (APMC) in [25]). In general, these methods include semi-analytical calculations to mitigate the intra-step absorption problem and produce accurate results, even for high step sizes. In [26], we have considered a more fundamental problem, the so called negative absorption index (NAI) problem which is the main underlying reason behind the many large-step size effects including intra-step absorption.

The Effective Geometry Monte Carlo (EG-MC) method discussed in this work solves the intra-step absorption problem by exploiting the locality of the interactions between molecules and the receiver and performing a corresponding geometric modification in the diffusion channel. The method is easy to implement, intuitive and outperforms Monte Carlo simulations by at least an order of magnitude while not requiring any semi-analytical calculations in-between each iteration step. The improvements to the simulation frameworks introduced in the molecular communication literature [21], [24]–[26] so far mainly focused on fixing the absorption rate problem while not taking the absorption angle into account. Nevertheless, as shown in [27], the angular distribution of absorbed molecules is also important for decreasing inter-symbol interference (ISI), since ISI significantly hinders the communication capacity of the diffusion channel [28], [29]. In addition, multi-receiver/transmitter systems have also been extensively explored in the literature for similar purposes [30]–[35]. In such multi-transmitter/receiver communication channels, one requires information that is related to the incident angle – $\theta, \phi$ in a 3-D channel – of the molecules inside the channel, as it can be used to demodulate the transmitted signal and the original transmitter from which the signal is received. In the context of a single spherical receiver, the angular information refers to the molecule absorption angle and can aid the receiver on locating the angular position of the transmitter [27]. Therefore, there is an urgent need in the literature for a reliable and efficient simulation framework that can take into account the angular effects as well. Furthermore, the mentioned simulation frameworks mainly focus on purely diffusive channels, whereas a more general method is required to incorporate the effect of flow inside the channel. In this paper, we build on [26] to show that the EG-MC algorithm indeed reproduces the absorption angle information quite accurately while performing better than traditional MC algorithm both in terms of computational power and accuracy. In doing so, we also lay stronger evidence for our claim that EG-MC indeed solves the NAI problem, since the average molecule absorption position becomes the surface of the boundary and the absorption angle is preserved. The molecules are absorbed in an effective way right at the receiver boundary along their path and upon collision, solving the problems that arise from finite step sizes. Moreover, we also show that EG-MC algorithm can be extended to molecular communication channels with constant flow, as long as the step-size ratio is small. Under this condition, EG-MC simulations match analytical results even for cases where the Peclet number is high, i.e. the motion of molecules is dominated by the flow.

The organization of this paper is as follows: In Section II, we consider a partially absorbing receiver inside a purely diffusive channel and summarize the EG-MC algorithm, which we first introduced in [26], with the addition of absorption angle detection code and give the analytical result for the angular distributions of the absorbed molecules [27], [36]. Afterwards, we compare the analytical solutions with MC and EG-MC simulations, showing the higher efficiency and accuracy of the EG-MC algorithm. Later, we perform error analysis to find the range of applicability for the algorithm. In Section III, we focus on an extension of the EG-MC algorithm to incorporate flows inside molecular communication channels. We use two illustrative examples as a proof of concept, to present our findings: an infinite planar receiver and a spherical absorbing receiver with constant flow. Finally, we conclude with possible future applications of our method and further computational opportunities that EG-MC method opens due to its high efficiency. In addition, we present a review for the EG-MC algorithm [26] in the Appendix while explaining the technical steps taken in its implementation. Throughout the paper, unless otherwise stated, the units in the figures and illustrations are $\mu m$, $s$, $\mu m^2/s$ for length and time scales, and diffusion coefficients, respectively. Both MC and EG-MC simulations are performed with an initial release of $10^5$ particles while using `SciPy` and `NumPy` libraries in the `Python` programming language.

## II. ANGULAR INFORMATION PRESERVATION FOR A SPHERICAL RECEIVER

### A. SYSTEM MODEL AND EG-MC ALGORITHM

In this section, we discuss a diffusion channel consisting of a spherical absorbing receiver with radius $R$ and a point transmitter located $L$ away from the origin in a 3-D unbounded environment. The system model is depicted in Fig.1 (left). The motion of the released molecules inside the diffusion channel is modeled by Brownian Motion as

$$\Delta x \sim \mathcal{N}(0, 2D\Delta t), \tag{1a}$$
$$\Delta y \sim \mathcal{N}(0, 2D\Delta t), \tag{1b}$$
$$\Delta z \sim \mathcal{N}(0, 2D\Delta t), \tag{1c}$$

where $D$ is diffusion coefficient, $\Delta x$, $\Delta y$ and $\Delta z$ are the single-step sizes in the three dimensions, $\Delta t$ is the time step, and $\mathcal{N}(\mu, \sigma^2)$ is the normal distribution with mean $\mu$ and variance $\sigma^2$. In a traditional MC algorithm, free diffusion is the first part of a single step. This is followed by the absorption of molecules within the receiver boundary. However, as

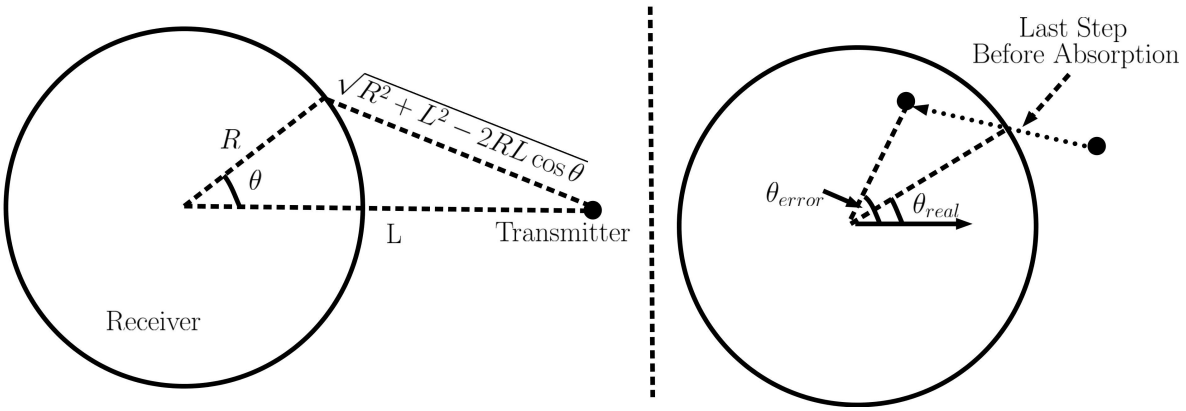


**FIGURE 1.** A diffusion channel consisting of a spherical absorbing receiver of radius $R$ concentric with the coordinate system and a point transmitter situated at $x = L$ (left); the systematic absorption angle shift of the traditional MC algorithms illustrated (right).

indicated in Fig. 1 (right), this absorption is likely to cause a systematic shift at higher angles (defining the angular position of the transmitter as zero) due to finite step size effects. The EG-MC method, described in algorithm 1, solves this problem by adding a thickness to the spherical receiver. Many absorption rate-related aspects of this algorithm are already illustrated in [26] and reviewed in the appendix. Therefore, we shall focus on its angular accuracy for this paper.

**Algorithm 1** Effective Geometry Monte Carlo (EG-MC)

**procedure** Absorption and Angle Detection($x_i$ for i=1,2,3)
  Define iteration number, initial position and simulation parameters ($D$,$L$,$\Delta t$)
  $t_f = \Delta t \times$ iteration
  **for** i = 1:iteration **do**
    Perform Diffusion Simulation
    $r = \sqrt{x^2 + y^2 + z^2}$
    index=find($r < R + \alpha\sqrt{D\Delta t}$)
    $N_{\text{abs}}$(i)= length(index) ▷ Number of absorbed particles
    (x,y,z)[index]=[] ▷ Molecules are absorbed
    Angle detection algorithm (See main text)
  **end for**
  **return** $N_{\text{abs}}$

One important addition we included in the EG-MC algorithm is the angle detection part. Assuming that the transmitter is situated at $x = L$ and defining $\hat{v}$ as the unit vector in the direction of the absorption position of the molecules and $\hat{x}$ as the unit vector in x-direction, the angle of absorption can be given as

$$\hat{v} \cdot \hat{x} = v_x = \cos\theta |\hat{v}||\hat{x}| \implies \theta = \arccos(v_x), \tag{2}$$

where $|\hat{v}| = |\hat{x}| = 1$ by construction.

### B. COMPARISON WITH ANALYTICAL RESULTS

Here, we perform comparisons of EG-MC and MC simulations with analytical results. Unfortunately, no exact results exist for angular distributions of the absorbed particles at a given time, only an asymptotic result for $t \to \infty$ [36] is available. In 3-D, the marginal angular distribution for the absorbed particles, $p(\theta, t \to \infty)$, can be given as [27]

$$p(\theta, t \to \infty) = \frac{R \sin\theta \left(1 - \frac{R^2}{L^2}\right)}{2L\left(1 - \frac{R}{L}\cos\theta + \frac{R^2}{L^2}\right)^{\frac{3}{2}}}. \tag{3}$$

Here $\int_0^\pi p(\theta, t \to \infty)\, \mathrm{d}\theta = \frac{R}{L}$ is the probability of eventual absorption of the released particle in a single particle experiment [10], where we emphasize that $0 < R/L < 1$. Comparing using this asymptotic result requires high computational power and would always include systematic errors.

Fortunately, Akdeniz *et al.* [27] derive an analytical approximation for the marginal angular distribution $p(\theta, t)$ for finite times, see their Eq. (16). According to the approximations performed in this work, $p(\theta, t)$ performs very well for $L \gg R$. In Fig. 2, we show, using small step size simulations, that this analytical approximation indeed requires that the initial position of the transmitter is far away. When using this formula for comparison, we impose the condition $L/R \geq 2.5$, which has been shown to be sufficient for comparisons in this paper.

Now, we shall start comparing the angular distributions obtained using the MC and EG-MC methods. We first define $\beta = \sqrt{2\,D\Delta t}/R$ as the ratio of position step-size to the radius of the receiver and set the free parameter of our EG-MC algorithm, $\alpha$, to 0.82 as we argued in [26]. In the following section, where we perform error analysis, we discuss the robustness of this value in further detail as well. In Fig. 3, the comparison between the analytical result and simulations has been illustrated for two different scenarios. As can be seen from the figure, EG-MC algorithm outperforms MC

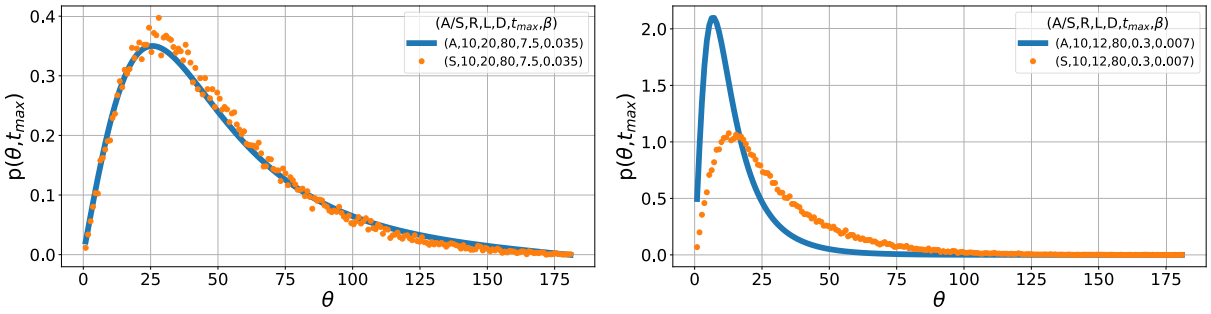


**FIGURE 2.** Comparison between the analytical result and simulations for small step sizes, for which MC and EG-MC algorithms closely agree. As can be seen from the figure, the analytical result found in [27] is not a good approximation for $L/R \leq 2$.

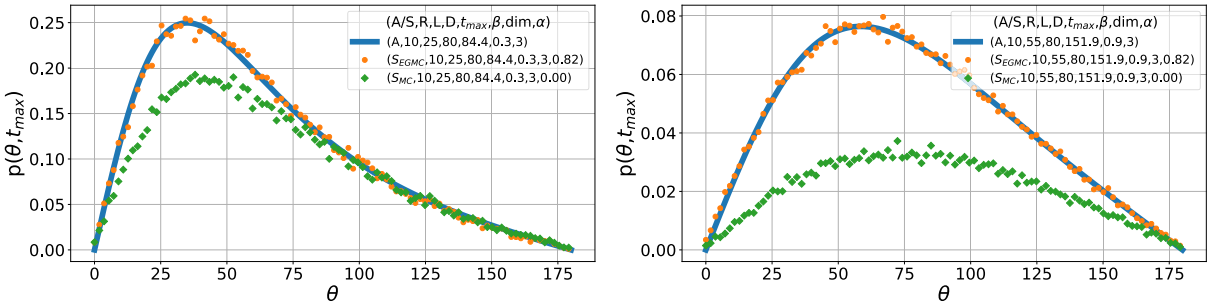


**FIGURE 3.** Comparison between the analytical result and simulations for 3-D unbounded channel. The EG-MC algorithm clearly preserves the angular information and outperforms the MC algorithm.

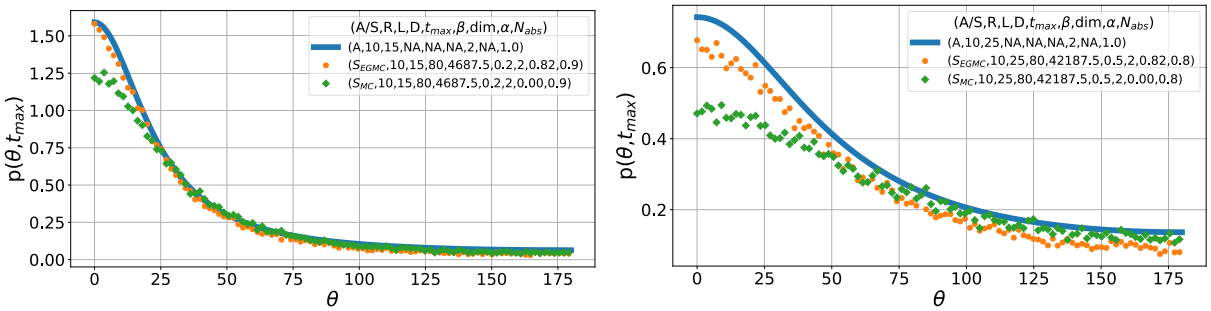


**FIGURE 4.** Comparison between the analytical asymptotic (as $t \to \infty$) result and large time simulations for 2-D unbounded channel. The difference between the asymptotic result and EG-MC simulation is independent of angle as expected, whereas a systematic shift to higher angles is observed for MC simulations.

simulations and does not suffer from systematic angle shifts observed for the MC algorithm.

The systematic angle shift is more obvious if one considers the 2-D case. The asymptotic solution for this case is also known [36], where all particles are absorbed by the receiver for large times. One important property of the diffusion is the fact that particle absorption at asymptotically large times is angle-independent, meaning that, at these times, particles are absorbed with equal probability at all angles. This suggests that the difference between the analytical result and the simulation result for $p(r, t)$, where $t$ is large, should be angle independent. This is the case for the EG-MC algorithm as can be seen from the Fig. 4, whereas the MC simulations show an apparent systematic shift in the angle distribution as expected.

From this point of view, the EG-MC algorithm not only outperforms MC-algorithm by at least an order of magnitude in terms of computation power (while giving a significantly more accurate absorption probability, as shown in [26]), but also predicts the absorption angle precisely within random simulation errors, as opposed to the MC algorithm which suffers from a systematic bias towards high angles. In the following section, we quantify this improvement by performing error analysis.

### C. ERROR ANALYSIS

In this section, we will answer two questions: Firstly, how does the EG-MC algorithm perform in comparison

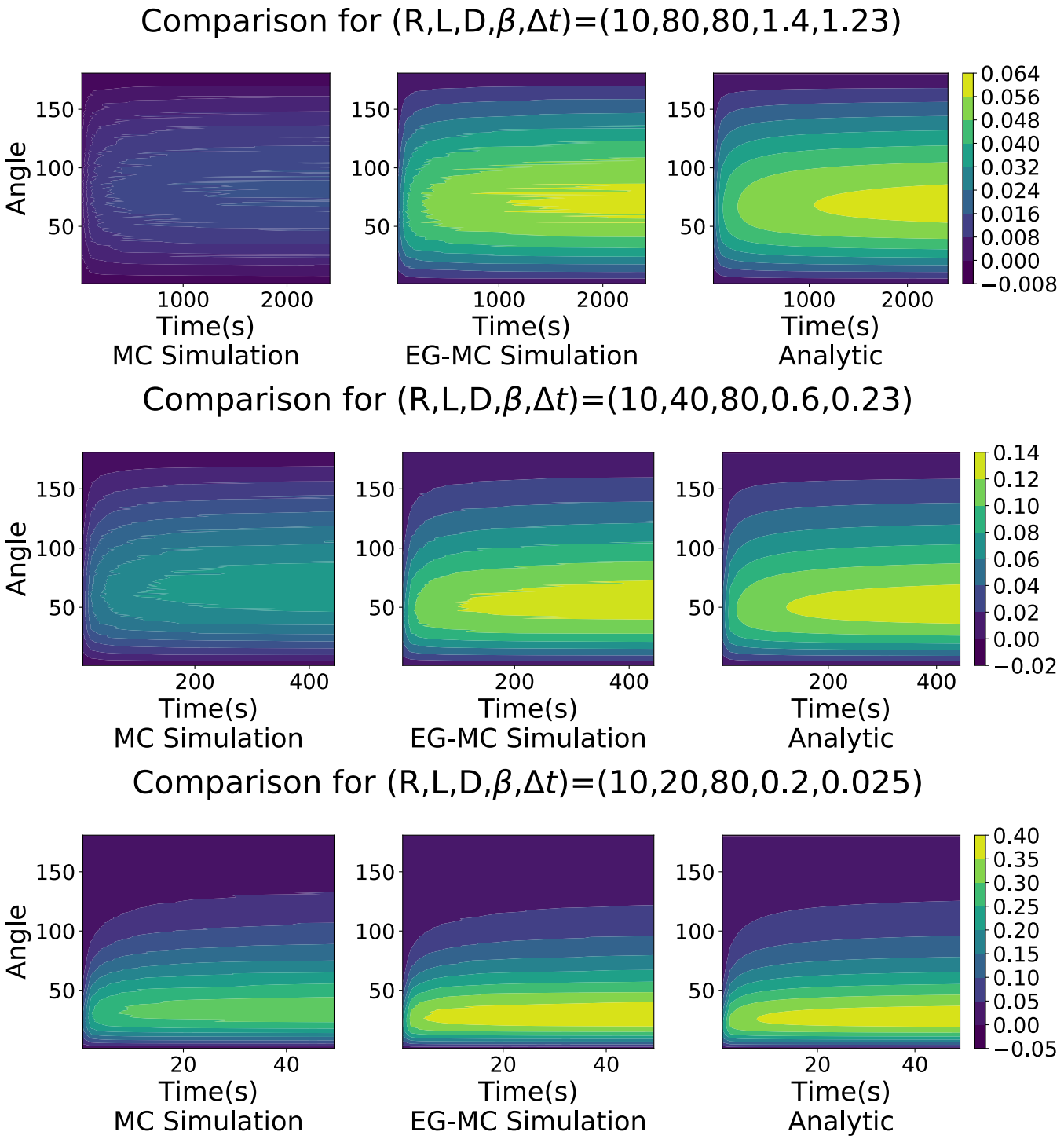


**FIGURE 5.** Comparison of $p(t,\theta)$ for analytical and simulation results for different times $t$ and angles $\theta$. Note that MC algorithm clearly shows a systematic error where first a less fraction of particles are absorbed at a given time and second a systemic shift to higher angles is observed.

to an MC-implementation (with $\alpha = 0$), and what is the optimal value of $\alpha$ if we want to reproduce the angular distribution as accurately as possible? Secondly, what are the limitations of the EG-MC method? First, we shall define a few important quantities that will be used in this analysis.

The relative error between the analytical result and the simulation result is defined as

$$e_{\text{rel}} = \frac{p^S(\theta,t) - p^A(\theta,t)}{p^A(\theta,t)}. \tag{4}$$

Moreover, the fraction of particles absorbed within the angle range $[0,\phi]$ until time $t$ by the receiver can

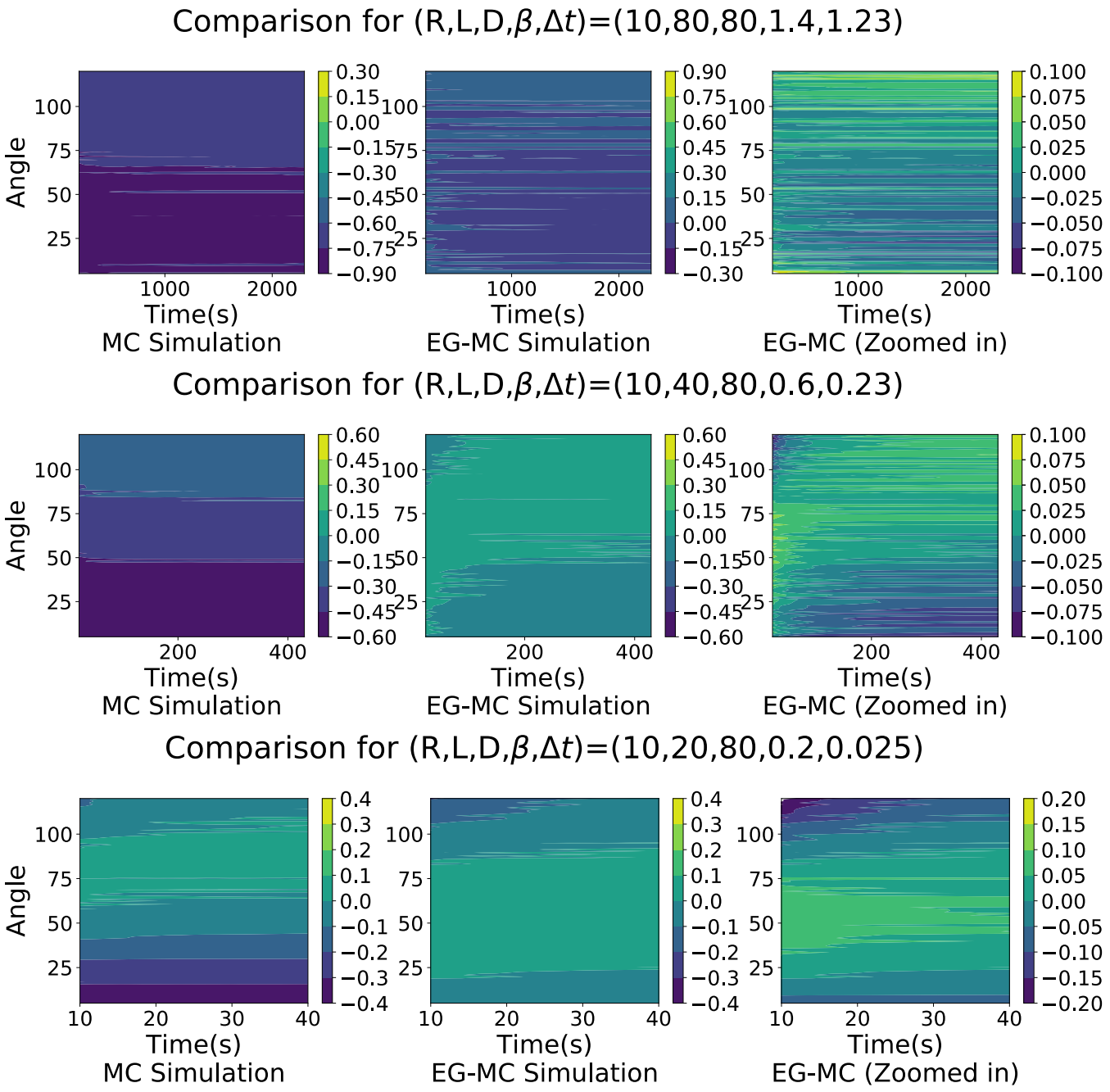


**FIGURE 6.** Comparison of relative error, $e_{\text{rel}}$, for analytical and simulation results at different times $t$ and angles $\theta$. We stress that the color bar scale (and the color tone) is the same for the first two figures, where the MC algorithm has an error within $(-0.8, -0.9)$ interval and therefore the color range seems different. For the first two rows, we notice that MC algorithm shows a color gradient, illustrating the systematic error inherent in the algorithm. On the other side, the EG-MC algorithm shows a random error confined within $|e_{\text{rel}}| \leq 0.1$. The final case is $R/L = 2$, and therefore the analytic result is not valid anymore, as is apparent from the color gradient in the EG-MC algorithm. In this manner, EG-MC algorithm can be an indicator for the cases where the analytical approximation of [27] fails to be precise.

be given as

$$F(\phi, t) = \int_0^{\phi} p(\theta, t)\, \mathrm{d}\theta, \tag{5}$$

where for $\phi = \pi$, $F(\pi, t)$ is the fraction of particles absorbed until time $t$.

Now, we start by illustrating the comparison between the analytical result and EG-MC and MC simulations in Fig. 5. In order to assess the performance of our algorithm, we use the relative error $e_{\text{rel}}$ defined above. This quantity is plotted in Fig. 6 for different choices of parameters. Note that for easy comparison between the MC and EG-MC performances the first two heatmaps in each row are plotted on the same scale, whereas in order to distinguish finer features in the EG-MC error the last plot in each row is a zoomed-in version

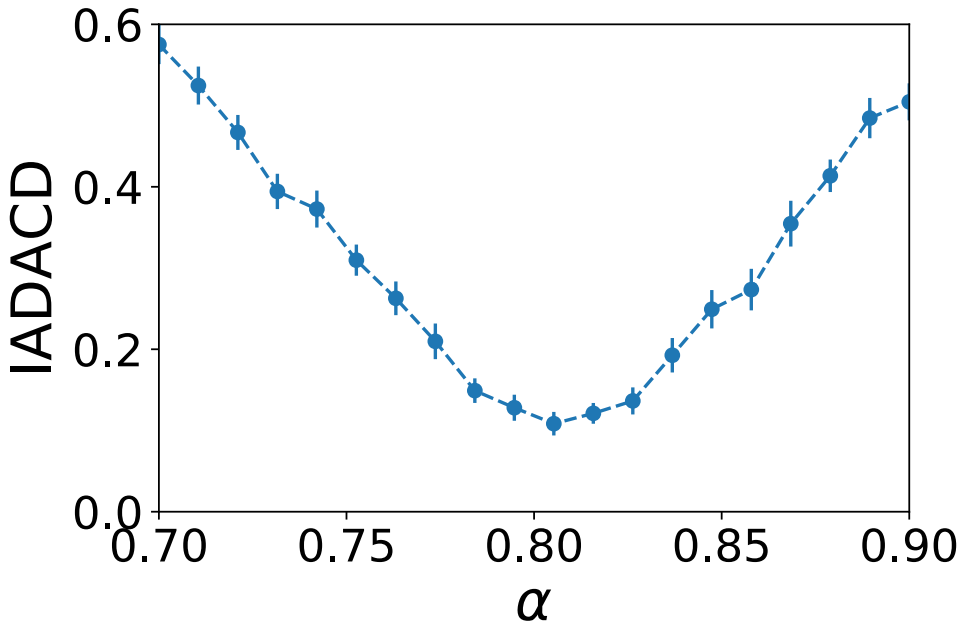


**FIGURE 7.** The IADACD as defined in Eq. 6 versus the free parameter $\alpha$. Each datapoint corresponds to an average of 30 runs of the simulation, errorbars are assigned as $\sqrt{(\text{Var}/30)}$, for $D = 80\mu m^2/s$, $R = 10\mu m$, $L = 80\mu m$.

of the second one. Concentrating on the first two rows for the time being, we see that the MC simulation suffers from systematic underpredictions of the particle flux (which is related to the NAI problem considered in [26]), but it also shows a clear systematic error in dependence on angle. On the contrary, the EG-MC simulation shows little systematic biases. It may be noted that the relative error is largely independent of time, because at each point in time the plotted data depends on all previous times, which introduces large correlations. Nonetheless, we argue that the definition of relative error is reasonable, since the absolute number of particles per unit angle received until a given time is the practically most important quantity. Furthermore, working with this quantity helps reduce the random error inevitably encountered in the simulation.

It can be seen that the situation is different for the case plotted in the last row of Fig. 6. Here, the EG-MC simulation seems to show systematic errors as well. This apparent failure, however, is due to the limits of applicability of the analytic result, and the EG-MC result is in fact more accurate.

In order to decide on the optimal choice of the parameter $\alpha$, we use a similar metric to the one introduced in [26]. We define the integrated absolute difference in the angular cumulative distribution (IADACD) as

$$\text{IADACD} = \sum_i |(F^S(\theta_i, t) - F^A(\theta_i, t))|, \tag{6}$$

where the sum runs over all angles in the interval $[0, \pi]$ for a given time $t$, and "S" and "A" denote the simulated and analytical results respectively. We evaluate this quantity at the maximum time in a given simulation.

Fig. 7 shows the IADACD as a function of $\alpha$. We observe that a value of $\alpha \sim 0.8$ minimizes the IADACD, which agrees with the results found in [26]. We note that in our previous work a more elaborate analysis was performed to find the optimal $\alpha$, but since we have confidence in the physical intuition underlying the EG-MC algorithm we take the results plotted in Fig. 7 as sufficient confirmation that the value of $\alpha$ optimizing the accuracy of the hitting rate does in fact also maximize the precision of the angular distribution.

We now turn to the second question posed at the beginning of this section, to wit, at which point the EG-MC algorithm has its limitations. It is clear that given a certain geometry the primary point of concern is the relationship between the typical stepsize encountered in the simulation and the extent of the receiver. Therefore, we use the dimensionless quantity $\beta = \sqrt{(2D\Delta t)}/R$ defined before and study the performance of the EG-MC algorithm in dependence on this parameter.

We define a comparison metric called relative inaccuracy as follows

$$\text{Relative inaccuracy} = \frac{\int_0^\pi (p^S(\theta, t) - p^A(\theta, t))^2 \, \mathrm{d}\theta|_{\alpha=0.8235}}{\int_0^\pi (p^S(\theta, t) - p^A(\theta, t))^2 \, \mathrm{d}\theta|_{\alpha=0}}. \tag{7}$$

In Fig. 8, we plot this quantity as a function of $\beta$ for a number of different cases. We observe that the general behavior of the relative inaccuracy is a constant value for low $\beta$ and then a steadily increases. The cutoff-value at which the relative inaccuracy starts to rise can – to a good approximation – be given by $\beta_0 = \min[2, (L - R)/2R]$. The first limit $\beta < 2$ is directly related to the geometry of the receiver, since if

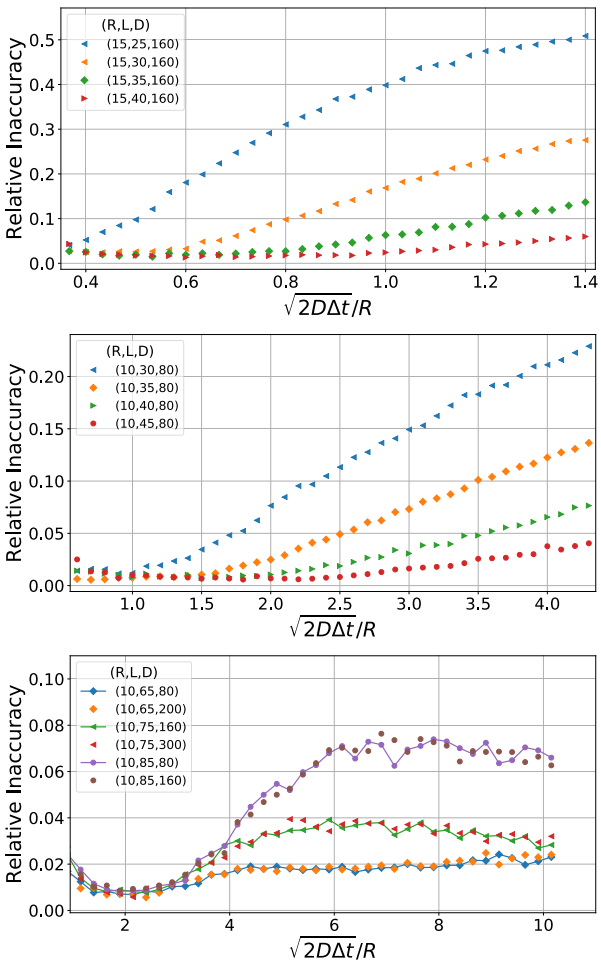


**FIGURE 8.** Illustration of relative inaccuracy as defined in Eq. (7) for various cases. Note that $\beta < (L-R)/2R$ and $\beta \leq 2$ is a reasonable condition for EG-MC algorithm to outperform significantly. We note that the relative inaccuracy is fairly independent of diffusion coefficient, $D$, as expected, since $D$ is simply a scaling of time.

the stepsize becomes comparable to the receiver's diameter any algorithm clearly runs into problems. On the other hand, the second limit $\beta < (L-R)/2R$ stems from the locality property extensively discussed in [26] which is of pivotal importance for the self-consistency of the EG-MC algorithm. If this bound is exceeded, the effective displacement of the receiver boundary changes the distribution of particles near the boundary to such an extent that the linear behavior of the expected absorption position on the boundary displacement is no longer preserved. Needless to say, the standard MC algorithm would fail miserably in the regions where EG-MC finds its limitations.

To return to the two questions posed at the beginning of this section, we conclude that the answers are very similar to the ones given in [26]. The EG-MC algorithm outperforms a standard MC implementation significantly in terms of accuracy in reproducing the correct angular distribution. Furthermore, the value of $\alpha$ found before is consistent with the simple test performed in this work. The limitations of the EG-MC algorithm are, as expected, closely connected to the problem of locality, and therefore very similar to the ones given in [26].

## III. BEYOND EG-MC: POSSIBLE EXTENSIONS FOR FLOW CHANNELS

In this section, we present a possible extension of the EG-MC algorithm to two simple molecular communication channels in the presence of flow. First, we consider the simplest case where an infinite planar receiver is situated $L$ away from the transmitter and there is a constant flow $v$ towards the receiver. Then, we show a simplified version of an unbounded channel with a spherical receiver and a constant flow, where we neglect the edge-effects on the flow that are caused by the existence of the spherical receiver. Both cases are presented as a proof of concept for the efficiency and effectiveness of the EG-MC algorithm even in the presence of flow.

In order to quantify whether diffusion or the flow is dominant in the channel, we first define the dimensionless Peclet number as

$$P_e = \frac{Lv}{D}, \tag{8}$$

where $L$ is the length of interest and will be taken as the distance of the transmitter from the origin from now on. A high $P_e$ implies that the diffusion is insignificant with respect to drift ($P_e \to \infty$ as $v \to \infty$), whereas for a low $P_e$, diffusion is more dominant ($P_e \to 0$ as $v \to 0$).

The first possible assumption for the range of applicability of the EG-MC algorithm in flow channels would be to constrain the Peclet number to be low, e.g. $P_e \ll 1$. Nonetheless, this is not required and the EG-MC algorithm is capable of performing precisely for high $P_e$ as we shall show shortly.

The metric that affects the performance of the EG-MC algorithm is the "step-size ratio" (SSR), which we define as follows

$$SSR = \frac{\Delta x_{\text{diffusion}}}{\Delta x_{\text{drift}}} = \frac{\sqrt{2D\Delta t}}{v\Delta t} = \sqrt{\frac{2D}{v^2\Delta t}}. \tag{9}$$

SSR is a measure of the ratio between the diffusion and drift space step sizes for a given time step $\Delta t$. Essentially, the EG-MC algorithm neutralizes the systemic errors of diffusion that arise due to finite step size. Thus, it is intuitively expected that SSR is the main measure of the accuracy for the EG-MC algorithm, not $P_e$. For the EG-MC algorithm to perform properly, we expect $SSR \gg 1$, such that the step size of diffusion outweighs that of drift. Nevertheless, we note that $P_e$ is an independent quantity and one can achieve high accuracy even for high $P_e$ as long as $\Delta t$ is properly tuned. Therefore, the EG-MC algorithm can sweep out the complete possible phase space for a given molecular communication channel in the presence of flow. Moreover, even if $SSR < 1$, as long as $\Delta x_{\text{drift}} \ll K$, where $K$ is the length scale of interest, the EG-MC algorithm converges to MC simulations and introduces no additional systematic error. For the remaining cases, a soft cut-off, $f(SSR)$, for the $\alpha$ value can be implemented using a function that is dependent only on SSR with the

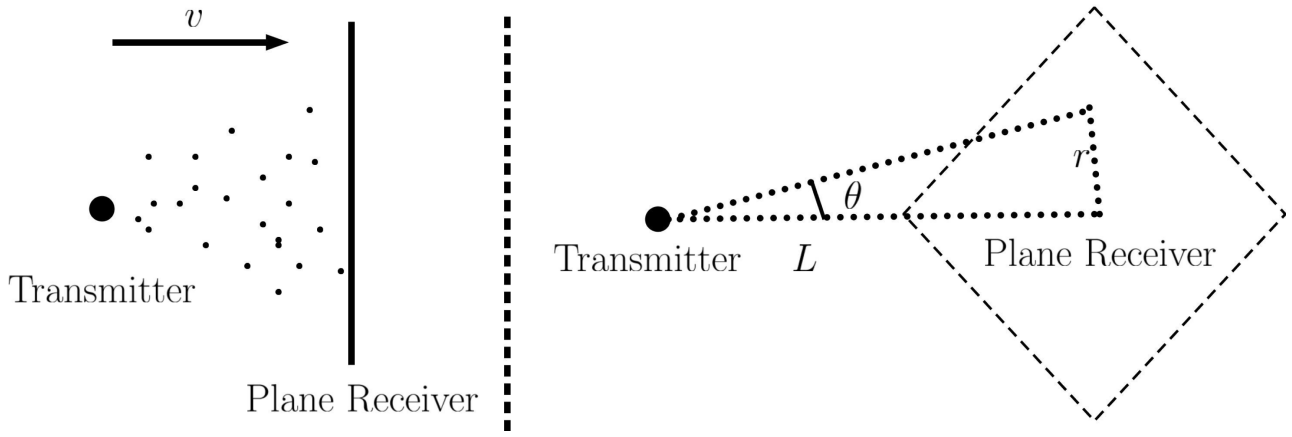


**FIGURE 9.** A model for a molecular communication channel with a plane receiver situated at $z = 0$, point transmitter at $z = L$ and a constant flow $v = -v\hat{z}$.

following form

$$f(x) = \begin{cases} 1 & x \gg SSR_c \\ 0 & x \ll SSR_c \\ \text{transition region} & \text{otherwise} \end{cases} \tag{10}$$

Then, the free parameter of the EG-MC algorithm can be replaced with $\alpha \rightarrow \alpha f(SSR)$ for maximum performance. An example of such a function is $f(x) = 0.5(1 - \tanh(g(SSR_{SSR_c - x.})))$, where $SSR_c$ is the cut-off value and $g$ is the a measure of how soft the cutoff is. We leave it to future work to determine the optimum function and parameters for the cut-off and focus on the cases where no cut-off is required. Moreover, we note that the MC algorithm is usually not the best option in such boundary cases either, so implementing this cut-off only prevents any systematic error that could stem from the EG-MC algorithm.

Throughout the rest of this section, we will only change the flow $v$ in our illustrations, since it helps emphasizing the change induced by this parameter and since we have already shown the consistency of EG-MC simulation for the rest of the parameters in the previous section and in [26].

### A. INFINITE PLANAR RECEIVER

Now we consider as a toy-model an infinite planar receiver embedded in a 3-D unbounded space with a constant flow $v$ towards the receiver, to validate our expectations from the EG-MC algorithm for the case $SSR \gg 1$. The system model for this channel is shown in Fig. 9. Here, the receiver is situated at $z = 0$ and the point transmitter is situated at $z = L$. The flow is in the $-z$ direction and can be given as $v = -v\hat{z}$, where $\hat{z}$ is the unit vector in the $z$ direction. The motion of the molecules can be modeled using a Gaussian distribution as in Eq. (II-A), this time with a mean of $-v\Delta t$ for the $z$-component as

$$\Delta x \sim \mathcal{N}(0, 2D\Delta t), \tag{11a}$$
$$\Delta y \sim \mathcal{N}(0, 2D\Delta t), \tag{11b}$$
$$\Delta z \sim \mathcal{N}(-v\Delta t, 2D\Delta t). \tag{11c}$$

The convection diffusion equation for this channel can be written as

$$\frac{\partial P(r,z,t)}{\partial t} = D\triangle P(r,z,t) + v\frac{\partial P(r,z,t)}{\partial z}, \tag{12}$$

where $P(r, z, t)$ is the probability density of a single molecule, $r = \sqrt{(x^2 + y^2)}$ and $\triangle$ is the Laplacian operator. The molecules are absorbed at the boundary $z = 0$ and are initially released from the position $(x, y, z) = (0, 0, L)$. This results in the following boundary conditions

$$P(r,z,t)|_{z=0} = 0 \tag{13a}$$
$$P(r,z,t)|_{t=0} = \delta(x)\delta(y)\delta(z-L). \tag{13b}$$

The solution to the one-dimensional case is already known and is given in [37]. A generalization of this result to 3-D is straightforward, where $P(r, z, t)$ can be given as in Eq. (14), as shown at the bottom of this page.

The hitting rate, $n_{\text{hit}}(t)$, for the messenger molecules can be defined as

$$n_{\text{hit}}(t) = \int_0^\infty 2\pi r \left.\frac{\partial P(r,z,t)}{\partial z}\right|_{z=0} \mathrm{d}r, \tag{15}$$

$$P(r,z,t) = \frac{e^{-\frac{r^2}{4Dt}}}{(4\pi Dt)^{3/2}}\left[\exp\left(-\frac{(z-L+vt)^2}{4Dt}\right) - \exp\left(-\frac{(z+L+vt)^2}{4Dt}\right)\exp\left(-\frac{vL}{D}\right)\right]. \tag{14}$$

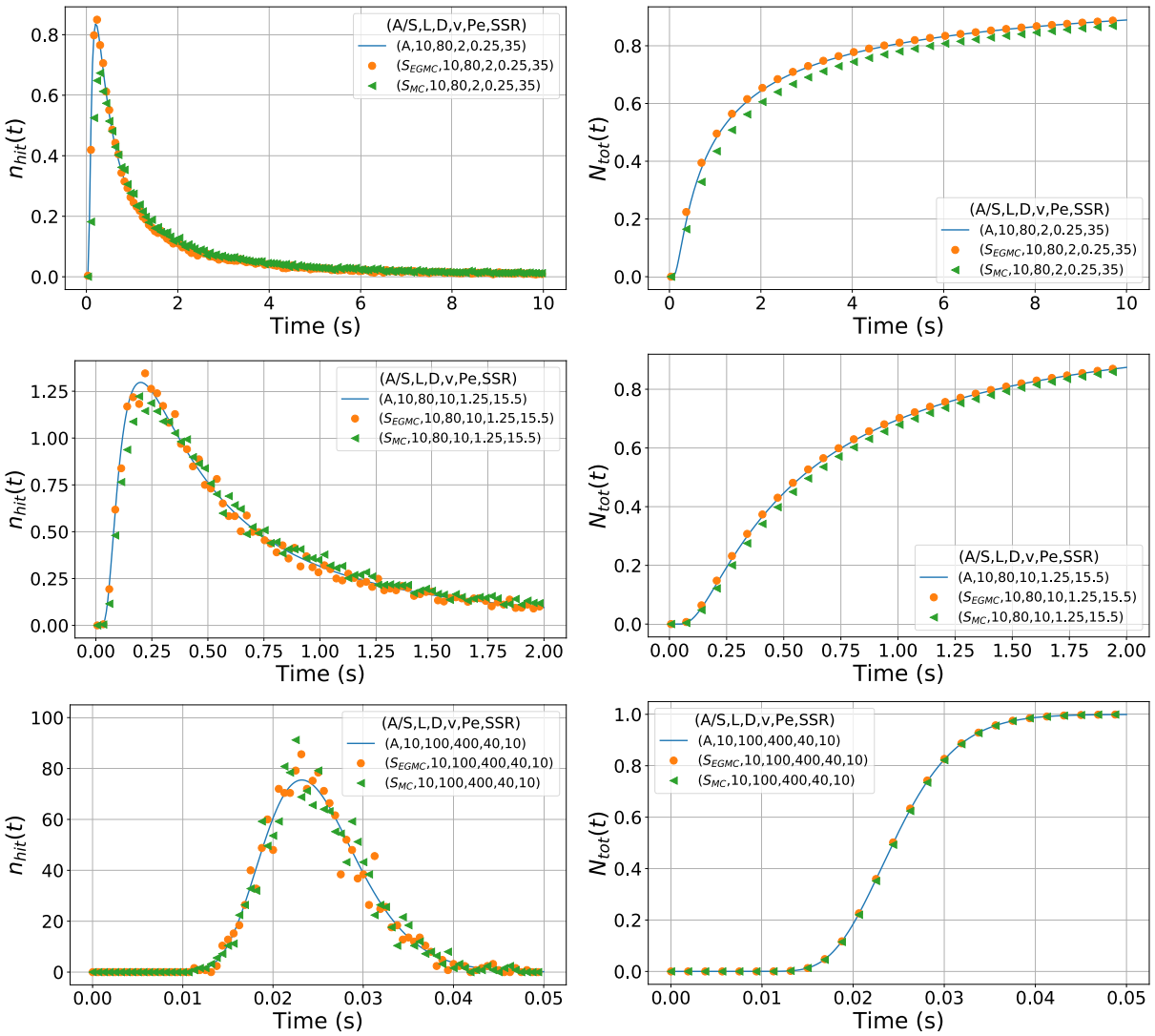


**FIGURE 10.** Illustration of the comparison of absorption information between the analytical result and EG-MC and MC algorithms for the plane receiver. As expected, EG-MC algorithm outperforms and is valid for the full range of $P_e$ as long as $SSR$ is large enough.

which is

$$n_{\text{hit}}(t) = \frac{L}{t\sqrt{4\pi Dt}} \exp\left(-\frac{(L-vt)^2}{4Dt}\right). \tag{16}$$

Then, the expectation value for the fraction of particles absorbed until time $t$, $N_{tot}(t)$, can be given as

$$N_{\text{tot}}(t) = \int_0^{\tau} n_{\text{hit}}(\tau)\,\mathrm{d}\tau. \tag{17}$$

We present the comparison of $n_{\text{hit}}(t)$ and $N_{\text{tot}}(t)$ between the analytical results and MC and EG-MC simulations in Fig. 10. As can be seen, the EG-MC algorithm precisely matches the analytical results within random errors whereas the MC-algorithm shows typical systematic errors discussed in [26]. As $P_e$ increases, the MC algorithm becomes more accurate as the drift motion becomes more dominant and the systematic errors inherent to the diffusion simulation become less significant.

We can define a marginal angular distribution, $p(\theta, t)$, for the fraction of particles absorbed until time $t$ as in the case of the partially absorbing spherical receiver inside a purely diffusive channel. We first realize that the fraction of molecules absorbed until time $t$ between radii $r$ (see figure 9, right) and $r + \delta r$ can be given as

$$p(r,t)\,\mathrm{d}r = 2\pi r \left.\frac{\partial P(r,z,t)}{\partial z}\right|_{z=0} \mathrm{d}r. \tag{18}$$

Then, using the definition $\tan\theta = r/L$, we arrive at $p(\theta, t)\,\mathrm{d}\theta$, such that $p(\theta, t)$ is the marginal angular distribution for the fraction of molecules that are absorbed by the receiver until time $t$, completely analogous to [27, eq. (16)]. Then, the cumulative angular distribution can be given as

$$F(\theta, t) = \int_0^{\theta} p(\phi, t)\,\mathrm{d}\phi, \tag{19}$$

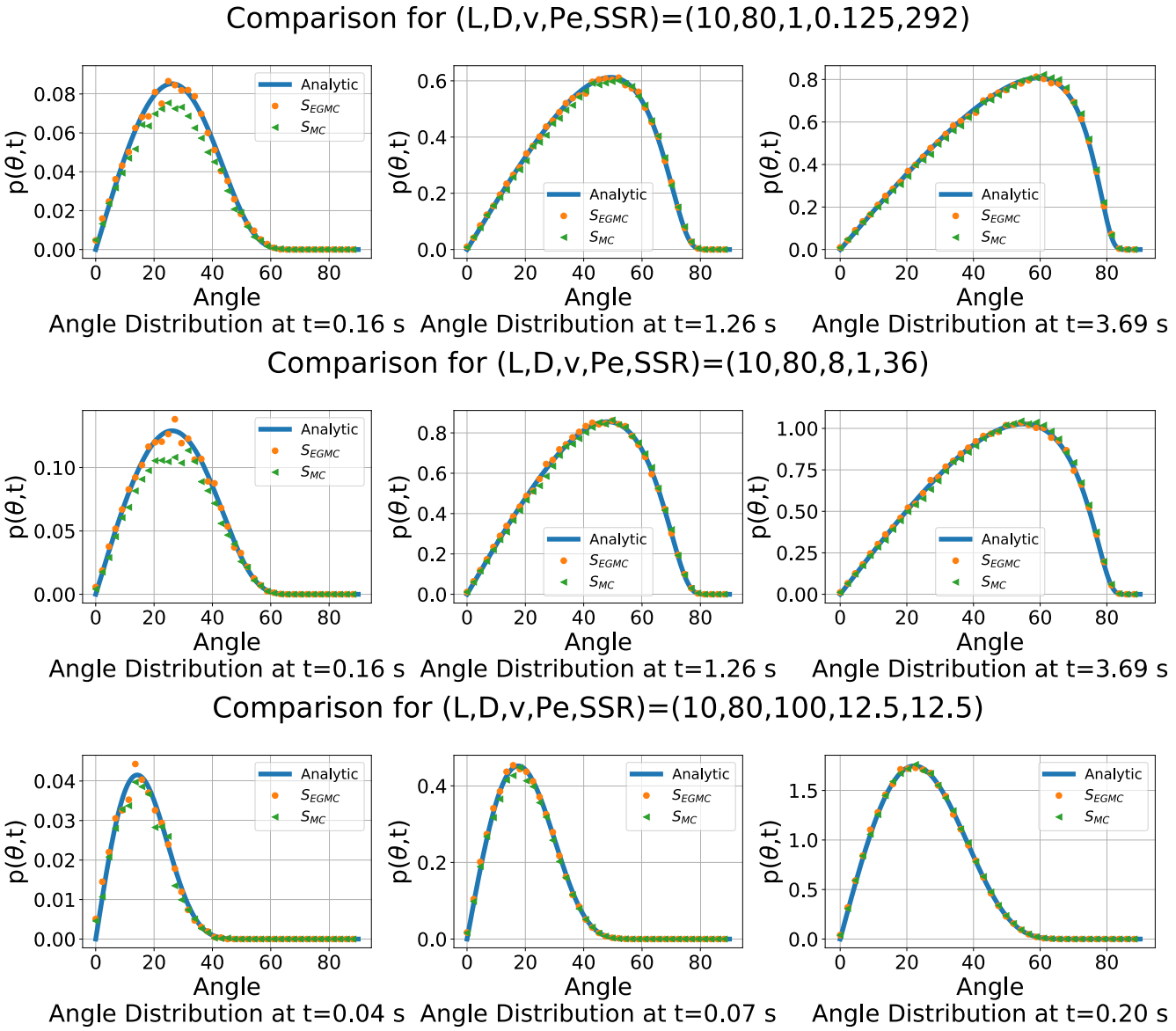


**FIGURE 11.** Illustration of the comparison of angular distribution between the analytical result and EG-MC and MC algorithms for the plane receiver. As expected, EG-MC algorithm outperforms and preserves the angular symmetry while being valid for the full range of $P_e$ as long as *SSR* is large enough.

where we realize that $F(\pi/2, t) = N_{\text{tot}}(t)$. We present the comparison of $n_{\text{hit}}(t)$ and $N_{\text{tot}}(t)$ between the analytical results and MC and EG-MC simulations in Fig. 11. As can be seen from the figure, the EG-MC algorithm precisely preserves the angular information in the system, whereas the MC-algorithm is inaccurate for low times. In contrast to a spherical receiver discussed in the previous section (see Fig. 1), the MC algorithm does not suffer from an apparent systematic shift to higher angles in the planar receiver case. This is mainly due to the fact that the absorption plane (defined in $x$-$y$ plane) and the absorption direction (perpendicular to $x$-$y$ plane at all points) are always perpendicular and the absorption plane has zero curvature. The main cause of error in MC simulations for the small times is the inaccuracy in $N_{\text{tot}}(t)$, as for larger times the MC simulation converges to the analytical solution without any shift to higher angles.

### B. SPHERICAL ABSORBING RECEIVER

As illustrated in the previous simple example, the EG-MC algorithm matches the analytical result within random errors and preserves the angular information in the presence of the flow, even for high $P_e$ for a planar surface. We can now consider a curved surface, namely the case of partially absorbing spherical receiver in the presence of a constant flow $v$. The system model is very similar to Fig. 1, with the only exception of a constant flow in the direction pointing from the transmitter to the receiver. Here, our main purpose is to illustrate that the EG-MC algorithm preserves the absorption

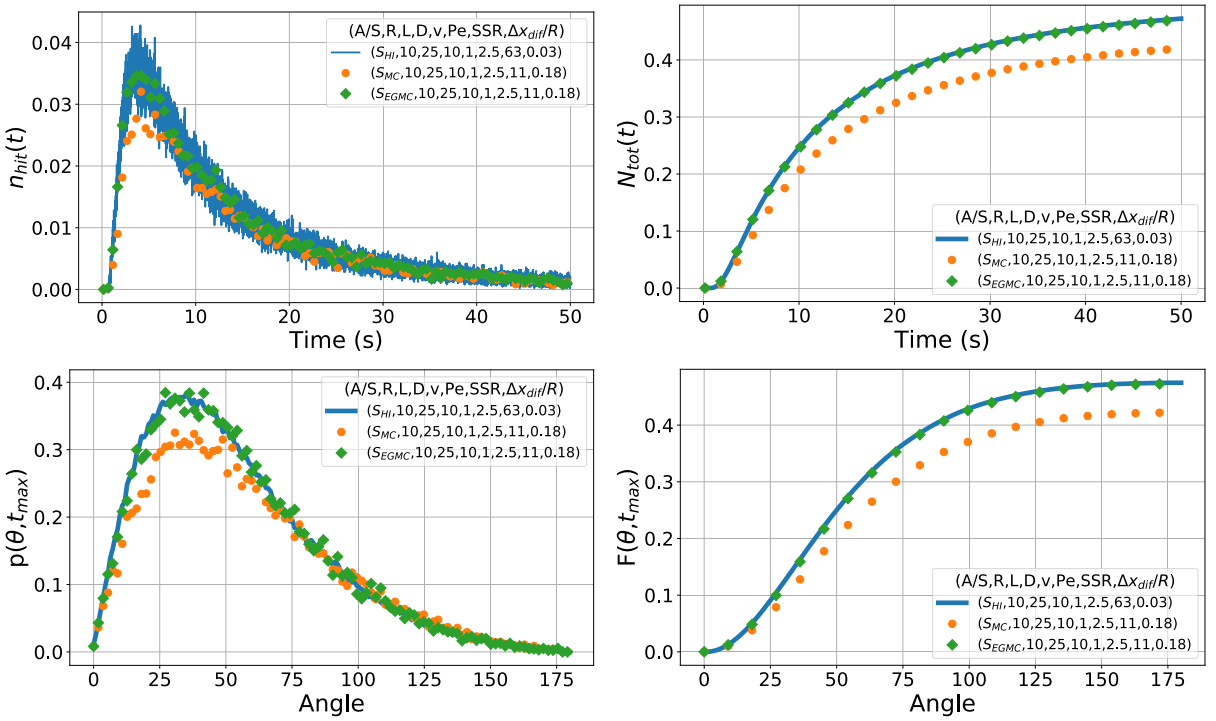


**FIGURE 12.** Comparison between $S_{HI}$, EG-MC and MC simulations for a flow velocity of $v = 1$ for the spherical absorbing receiver. Note the preciseness of EG-MC algorithm for each measure.

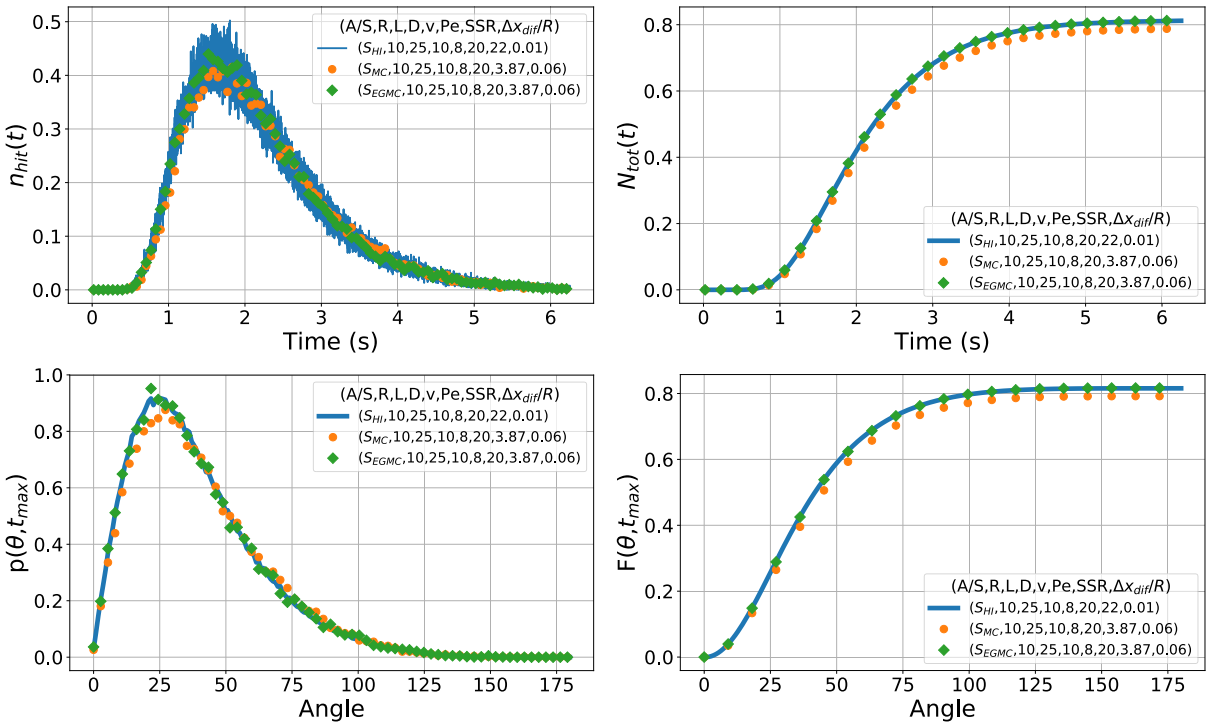


**FIGURE 13.** Comparison between $S_{HI}$, EG-MC and MC simulations for a flow velocity of $v = 8$ for the spherical absorbing receiver. Note the preciseness of EG-MC algorithm for each measure.

rate and angular information in the presence of a flow even for a spherical receiver. Therefore, for simplicity, we assume that the presence of the sphere does not change the flow, even though it does. The analytical result for this channel will be approximated using a simulation with a very small step size, hence high iteration number, and will be denoted as $S_{HI}$.

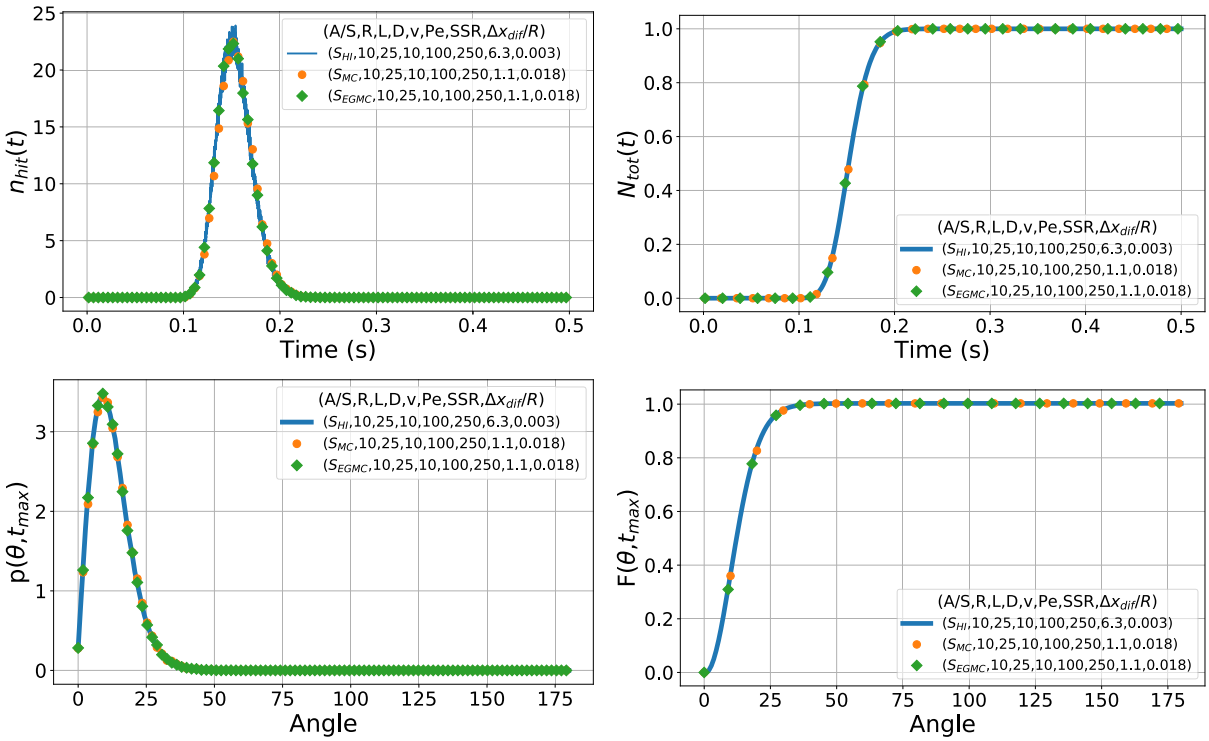


**FIGURE 14.** Comparison between $S_{HI}$, EG-MC and MC simulations for a flow velocity of $v = 100\mu m/s$ for the spherical absorbing receiver. Note that as $P_e$ is very large, the systematic shift caused by diffusion is now negligible, hence both EG-MC and MC perform significantly well.

The results we show in this section are approximate and should be interpreted only for the sake of illustration of the accuracy of the EG-MC algorithm.

As before, we shall use the hitting rate, $n_{\text{hit}}(t)$, the expectation value for the fraction of absorbed particles until time $t$, $N_{\text{tot}}(t)$, marginal angular distribution, $p(\theta, t)$ and the cumulative angular distribution $F(\theta, t)$ for comparison purposes. In Figs. 12, 13 and 14, the comparison between $S_{HI}$ and the MC and EG-MC simulations is given for $v = 1\mu m/s$, $v = 8\mu m/s$ and $v = 100\mu m/s$, respectively. As can be seen from the figures, the MC algorithm suffers from the systematic shift to higher angles for low $v$-values as described before, whereas the EG-MC algorithm matches $S_{HI}$ within random errors. For high $v$-values, the drift is dominant and the systematic error caused by diffusion is negligible as shown in Fig. 14. We note that $N_{\text{tot}}(t)$ and $F(\theta, t)$ serve as better indicators for systematic errors, as the random error on $n_{\text{hit}}(t)$ and $p(\theta, t)$ is summed over multiple data points. We conclude this section by emphasizing that a more precise simulation can be performed by taking into account the edge-effects caused by the spherical receiver that change the uniform flow in the close neighborhood of the receiver as long as $SSR \gg 1$; but this complication is out of scope of our treatment as we simply present a proof of concept.

## IV. CONCLUSION

In this paper, we have built on [26] showing that the EG-MC algorithm can at the same time precisely preserve the angular information of the absorbed molecules as well as their absorption probability. The angular information of the absorbed molecules is of immense importance, as, first, this information can be used to increase the signal to ISI ratio [27], and, second, it can benefit the receiver in distinguishing between transmitters which are situated at different locations in the channel. We performed extensive error analysis to show that the EG-MC method which has been shown to be fast and reliable in terms of predicting the absorbed particle fraction [26], also preserves the angular information precisely and requires significantly lower simulation run-times compared to the traditional MC algorithm. We also show that the EG-MC algorithm out-performs the MC simulations and matches the analytical results accurately even in the presence of uniform background flow, provided the step-size ratio is high.

Until now, the MC algorithm has been the dominant and widely used algorithm in the literature. The reason for this phenomenon can be understood from two reasons. First, the MC algorithm is a reliable algorithm which converges to the analytic result as $\Delta t \to 0$. Second, the MC algorithm is easy to implement and works for a variety of systems without requiring any semi-analytic calculations, hence introducing no complexity to the problem other than the requirement that $\Delta t$ should be sufficiently small. In this paper and in [26], we showed that EG-MC algorithm has both of these qualities, while having better convergence properties than the MC algorithm and not suffering from the systematic error that

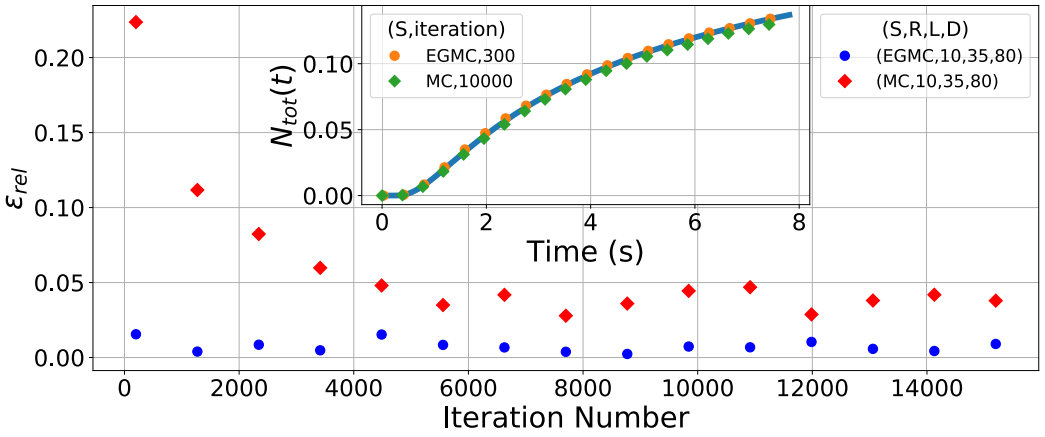


**FIGURE 15.** An illustration of the computational power of the EG-MC algorithm with respect to the traditional MC algorithm. Whereas the EG-MC algorithm describes $N_{\text{tot}}(t)$ quite accurately even for 300 iterations, MC algorithm cannot match the analytic result even for 10000 iterations.

MC has regarding absorption angles. As an improvement to many proposed simulation methods, such as [24] and [25], the EG-MC algorithm can easily be generalized to different shapes and multiple-receiver/transmitter systems and is the natural extension of the MC method. When simulating obstacle-rich environments, many proposed methods in the literature bring additional complexity with increasing number of obstacles, whereas with EG-MC simulations no additional complexity is introduced. Using a semi-analytic method in such cases may not be optimal as many semi-analytic methods require further calculations to implement, while EG-MC simply requires the same amount of coding as in the MC algorithm case.

Together with [26], we have concluded our analysis showing that the EG-MC algorithm outperforms the MC algorithm while retaining all of the benefits the MC method has for channels with a single receiver. The next natural line of research would be to first use the EG-MC algorithm in complex structures with noisy channels and acquire corresponding channel characteristics. The computational efficiency and reliability of the EG-MC method clear the way for a great number of future advances in the molecular communication literature.

## APPENDIX
## EFFECTIVE GEOMETRY MONTE CARLO ALGORITHM: REVIEW

In this section we shall review the key idea behind the EG-MC algorithm and illustrate its computational power over the traditional MC algorithm by showing example cases. For now, we review the concepts we introduced in [26] and discuss only angle-dependent impulse response of a spherical absorbing receiver situated in a 3-D unbounded channel. In the next section, we develop on this idea to show that EG-MC algorithm works perfectly accurate for the angle-dependent impulse as well.

The elegance of the EG-MC algorithm stems from its easy-to-implement nature, as it simply changes the geometry of the receiver while not requiring any computational implementation between diffusion steps. In doing so, the main pre-requisite is the assumption of the locality principle, which requires that the step-size of the diffusion should be smaller than the length scale of interest. This can be translated into mathematical language as discussed in section II, where we found that $\beta_0 = \min[2, (L-R)/2R]$ is a sufficient condition for the EG-MC algorithm to perform accurately.

After ensuring that the principle of locality holds, we simply change the radius of the receiver $R \to R + \alpha\sqrt{D\Delta t}$ as shown in Algorithm 1. Here, $\alpha$ is the free parameter of the theory and was found empirically to be $\sim 0.82$ in [26]. This linear increase in the receiver radius has been shown to solve the intra-step absorption problem. Moreover, as $\Delta t \to 0$, the MC and EG-MC algorithm converge to the same behavior. Now, we can focus on illustrating the computational power of the EG-MC algorithm.

In order to quantitatively compare both simulations, we first define the the probability that a released particle is absorbed in a single particle experiment until time $t$ as [10]

$$N^{A}_{\text{tot}}(t) = \int_0^t n_{\text{hit}}(\tau)\,\mathrm{d}\tau = \frac{R}{L}\operatorname{erfc}\left[\frac{L-R}{\sqrt{4Dt}}\right]. \tag{20}$$

Here, $A$ stands for the analytic result. Similarly, for EG-MC and MC methods, we will denote the simulation result as $N^{\text{EGMC}}_{\text{tot}}(t)$ and $N^{\text{MC}}_{\text{tot}}(t)$. Then, we define the average relative error for this case as

$$\varepsilon^{\text{EGMC}}_{\text{rel}} = \frac{1}{\text{iteration}} \sum_{t=\Delta t}^{t_{max}} \frac{|N^{A}_{\text{tot}}(t) - N^{\text{EGMC}}_{\text{tot}}(t)|}{N^{A}_{\text{tot}}(t)} \tag{21}$$

where we take $\Delta t = (L-R)^2/(D \times \text{iteration})$, the sum is over the discrete time values $(\Delta t, 2\Delta t, \ldots, t_{max} = \Delta t \times \text{iteration})$ and iteration denotes the total number of iterations performed in the particle based simulation. The relative error for the

MC algorithm can be defined analogously. We illustrate the computational efficiency and reliability of EG-MC algorithm in Fig. 15, where we plot the relative error for both algorithms versus the iteration number for channel parameters $R = 10\mu m$, $L = 35\mu m$ and $D = 80\mu m^2/s$. As can be seen from the figure, the EG-MC algorithm clearly outperforms the MC algorithm over all iteration numbers. It is important to note that usually the run-time of the simulation algorithm scales linearly with the total number of iterations. As can be seen from the figure, the EG-MC algorithm matches the analytic result clearly even for 300 iterations, whereas the MC algorithm struggles to match the analytic result at high iteration numbers such as 10000 while requiring 33-fold more computation time. Finally, we conclude this appendix by noting that we only illustrated the power of EG-MC algorithm for a single case as a more extensive discussion of this topic can be found in [26].

## ACKNOWLEDGEMENTS

*(Fatih Dinç, Matija Medvidović, and Leander Thiele contributed equally to this work.)* All authors would like to thank James Forrest, the Perimeter Scholars International program, and the University of Waterloo for the immense resources made available for this research. LT acknowledges support by the Studienstiftung des Deutschen Volkes.

## REFERENCES

[1] N. Farsad, H. B. Yilmaz, A. Eckford, C.-B. Chae, and W. Guo, "A comprehensive survey of recent advancements in molecular communication," *IEEE Commun. Surveys Tuts.*, vol. 18, no. 3, pp. 1887–1919, 3rd Quart., 2016.

[2] T. Nakano, M. J. Moore, F. Wei, A. V. Vasilakos, and J. Shuai, "Molecular communication and networking: Opportunities and challenges," *IEEE Trans. Nanobiosci.*, vol. 11, no. 2, pp. 135–148, Jun. 2012.

[3] W. Wicke, A. Ahmadzadeh, V. Jamali, H. Unterweger, C. Alexiou, and R. Schober. (2018). "Magnetic nanoparticle based molecular communication in microfluidic environments." [Online]. Available: https://arxiv.org/abs/1808.05147

[4] H. B. Yilmaz and C.-B. Chae, "Arrival modelling for molecular communication via diffusion," *Electron. Lett.*, vol. 50, no. 23, pp. 1667–1669, 2014.

[5] T. Nakano, Y. Okaie, and J. Q. Liu, "Channel model and capacity analysis of molecular communication with Brownian motion," *IEEE Commun. Lett.*, vol. 16, no. 6, pp. 797–800, Jun. 2012.

[6] D. Malak and O. B. Akan, "Molecular communication nanonetworks inside human body," *Nano Commun. Netw.*, vol. 3, no. 1, pp. 19–35, Mar. 2012.

[7] S. Hiyama and Y. Moritani, "Molecular communication: Harnessing biochemical materials to engineer biomimetic communication systems," *Nano Commun. Netw.*, vol. , no. 1, pp. 20–30, Mar. 2010.

[8] S. Hiyama, Y. Moritani, and T. Suda, "A biochemically-engineered molecular communication system (Invited Paper)," in *Nano-Net* (Lecture Notes of the Institute for Computer Sciences, Social Informatics and Telecommunications Engineering), vol. 3, M. Cheng, Ed. Berlin, Germany: Springer, 2009. [Online]. Available: https://link.springer.com/chapter/10.1007/978-3-642-02427-6_17#citeas

[9] T. Khan, B. A. Bilgin, and O. B. Akan, "Diffusion-based model for synaptic molecular communication channel," *IEEE Trans. Nanobiosci.*, vol. 16, no. 4, pp. 299–308, Jun. 2017.

[10] H. B. Yilmaz, A. C. Heren, T. Tugcu, and C.-B. Chae, "Three-dimensional channel characteristics for molecular communications with an absorbing receiver," *IEEE Commun. Lett.*, vol. 18, no. 6, pp. 929–932, Jun. 2014.

[11] M. M. Al-Zu'bi and A. S. Mohan, "Modeling of ligand-receptor protein interaction in biodegradable spherical bounded biological microenvironments," *IEEE Access*, vol. 6, pp. 25007–25018, 2018.

[12] Y. Deng, A. Noel, M. Elkashlan, A. Nallanathan, and K. C. Cheung, "Molecular communication with a reversible adsorption receiver," in *Proc. IEEE Int. Conf. Commun. (ICC)*, May 2016, pp. 1–7.

[13] M. Turan, M. S. Kuran, H. B. Yilmaz, I. Demirkol, and T. Tugcu, "Channel model of molecular communication via diffusion in a vessel-like environment considering a partially covering receiver," in *Proc. IEEE Int. Black Sea Conf. Commun. Netw. (BlackSeaCom)*, Jun. 2018, pp. 1–5.

[14] A. Noel and D. Makrakis. (2018). "Algorithm for mesoscopic advection-diffusion." [Online]. Available: https://arxiv.org/abs/1805.12438

[15] Y. Deng, A. Noel, W. Guo, A. Nallanathan, and M. Elkashlan, "Analyzing large-scale multiuser molecular communication via 3-D stochastic geometry," *IEEE Trans. Mol., Biol. Multi-Scale Commun.*, vol. 3, no. 2, pp. 118–133, Jun. 2017.

[16] T. Jahani-Nezhad and F. S. Tabataba. (2018). "Performance analysis of molecular spatial modulation (MSM) in diffusion based molecular MIMO communication systems." [Online]. Available: https://arxiv.org/abs/1809.05954

[17] S. Salehi, N. S. Moayedian, S. H. Javanmard, and E. Alarcón, "Lifetime improvement of a multiple transmitter local drug delivery system based on diffusive molecular communication," *IEEE Trans. Nanobiosci.*, vol. 17, no. 3, pp. 352–360, Jul. 2018.

[18] I. Llatser, D. Demiray, A. Cabellos-Aparicio, D. T. Altilar, and E. Alarcón, "N3Sim: Simulation framework for diffusion-based molecular communication nanonetworks," *Simul. Model. Pract. Theory*, vol. 42, pp. 210–222, Mar. 2014.

[19] E. Gul, B. Atakan, and O. B. Akan, "NanoNS: A nanoscale network simulator framework for molecular communications," *Nano Commun. Netw.*, vol. 1, no. 2, pp. 138–156, Jun. 2010.

[20] L. Felicetti, M. Femminella, G. Reali, P. Gresele, and M. Malvestiti, "Simulating an in vitro experiment on nanoscale communications by using BiNS2," *Nano Commun. Netw.*, vol. 4, no. 4, pp. 172–180, Dec. 2013.

[21] A. Noel, K. C. Cheung, R. Schober, D. Makrakis, and A. Hafid, "Simulating with AcCoRD: Actor-based communication via reaction–diffusion," *Nano Commun. Netw.*, vol. 11, pp. 44–75, Mar. 2017.

[22] Y. Jian *et al.*, "nanons3: A network simulator for bacterial nanonetworks based on molecular communication," *Nano Commun. Netw.*, vol. 12, pp. 1–11, Jun. 2017.

[23] H. B. Yilmaz and C.-B. Chae, "Simulation study of molecular communication systems with an absorbing receiver: Modulation and ISI mitigation techniques," *Simul. Model. Pract. Theory*, vol. 49, pp. 136–150, Dec. 2014.

[24] D. Arifler and D. Arifler, "Monte carlo analysis of molecule absorption probabilities in diffusion-based nanoscale communication systems with multiple receivers," *IEEE Trans. Nanobiosci.*, vol. 16, no. 3, pp. 157–165, Apr. 2017.

[25] Y. Wang, A. Noel, and N. Yang. (2018). "A novel a priori simulation algorithm for absorbing receivers in diffusion-based molecular communication systems." [Online]. Available: https://arxiv.org/abs/1809.00808

[26] F. Dinc, L. Thiele, and B. C. Akdeniz. (2018). "The effective geometry Monte Carlo algorithm: Applications to molecular communication." [Online]. Available: https://arxiv.org/abs/1809.06438

[27] B. C. Akdeniz, N. A. Turgut, H. B. Yilmaz, C.-B. Chae, T. Tugcu, and A. E. Pusane, "Molecular signal modeling of a partially counting absorbing spherical receiver," *IEEE Trans. Commun.*, vol. 66, no. 12, pp. 6237–6246, Dec. 2018.

[28] A. Noel, K. Cheung, and R. Schober, "Optimal receiver design for diffusive molecular communication with flow and additive noise," *IEEE Trans. Nanobiosci.*, vol. 13, no. 3, pp. 350–362, Sep. 2014.

[29] W.-A. Lin, Y.-C. Lee, P.-C. Yeh, and C.-H. Lee, "Signal detection and ISI cancellation for quantity-based amplitude modulation in diffusion-based molecular communications," in *Proc. IEEE Global Commun. Conf. (GLOBECOM)*, Dec. 2012, pp. 4362–4367.

[30] Y. Huang, M. Wen, L.-L. Yang, C.-B. Chae, and F. Ji. (2018). "Spatial modulation for molecular communication." [Online]. Available: https://arxiv.org/abs/1807.01468

[31] N. Pandey, R. K. Mallik, and B. Lall, "Molecular communication: The first arrival position channel," *IEEE Wireless Commun. Lett.*, to be published. [Online]. Available: https://ieeexplore.ieee.org/document/8510902

[32] M. J. Moore, T. Suda, and K. Oiwa, "Molecular communication: Modeling noise effects on information rate," *IEEE Trans. Nanobiosci.*, vol. 8, no. 2, pp. 169–180, Jun. 2009.

[33] M. J. Moore and T. Nakano, "Addressing by beacon distances using molecular communication," *Nano Commun. Netw.*, vol. 2, nos. 2–3, pp. 161–173, 2011.

[34] T. Nakano, Y. Okaie, and A. V. Vasilakos, "Transmission rate control for molecular communication among biological nanomachines," *IEEE J. Sel. Areas Commun.*, vol. 31, no. 12, pp. 835–846, Dec. 2013.
[35] S. S. Assaf, S. Salehi, R. G. Cid-Fuentes, and J. Solé-Pareta, and E. Alarcón, "Influence of neighboring absorbing receivers upon the inter-symbol interference in a diffusion-based molecular communication system," *Nano Commun. Netw.*, vol. 14, pp. 40–47, Dec. 2017.
[36] S. Redner, *A Guide to First-Passage Processes*. Cambridge, U.K.: Cambridge Univ. Press, 2001.
[37] S. Kadloor and R. Adve, "A framework to study the molecular communication system," in *Proc. 18th Int. Conf. Comput. Commun. Netw.*, Aug. 2009, pp. 1–6.

**FATIH DINÇ** received the B.S. degree in physics and in electrical and electronics engineering from Bogazici University, Turkey, in 2018. He is currently pursuing the master's degree with the Perimeter Institute for Theoretical Physics. His research interests include quantum information and quantum optics.

**MATIJA MEDVIDOVIĆ** received the master's degree in physics from the University of Zagreb, in 2017. He is currently pursuing the master's degree with the Perimeter Institute for Theoretical Physics. His research interests include condensed matter and computational physics.

**LEANDER THIELE** received the B.A. degree in physics in Oxford, U.K., in 2018. He is currently pursuing the master's degree with the Perimeter Institute for Theoretical Physics. His research interests include computational methods and statistics.